Journal of Organometallic Chemistry 743 (2013) 179–186

Contents lists available at SciVerse ScienceDirect

Journal of Organometallic Chemistry

journal homepage: www.elsevier.com/locate/jorganchem

On rhodium complexes bearing H-spirophosphorane derived ligands: Synthesis, structural and catalytic properties

Anna Skarżyńska*, Ewa Mieczyńska, Miłosz Siczek

Faculty of Chemistry, University of Wrocław, ul. F. Joliot-Curie 14, 50-383 Wrocław, Poland

ARTICLE INFO

Article history:
Received 16 April 2013
Received in revised form
13 June 2013
Accepted 18 June 2013

Keywords:
H-spirophosphorane ligands
Phosphorus ligands
Rhodium complexes
Hydroformylation reactions
Catalysis
X-ray structure

ABSTRACT

We investigated the coordination properties of H-spirophosphoranes towards rhodium ion. Symmetrical phosphorus ligands: $HP(OCH_2CH_2NH)_2$ **L1**, $HP(OCH_2CMe_2NH)_2$ **L2**, $HP(OCMe_2CMe_2O)_2$ **L3**, $HP(OC_6H_4NH)_2$ **L4**, and unsymmetrical phosphorus ligands: $HP(OCMe_2CMe_2O)(OCH_2CMe_2NH)$ **L5**, $HP(OCMe_2CMe_2O)(OC_6H_4NH)$ **L6** were found to coordinate to rhodium precursor $[Rh(CO)_2Cl]_2$ exclusively in protonated κ^2-P,E (E = N, O) bidentate fashion, yielding complexes [Rh(CO)Cl**L**] **1**–**6**. The complexes were characterised by spectroscopic methods. The molecular structures of the ligand **L6** complexes **3**, **5** and **6** were determined by single-crystal X-ray diffraction. The catalytic activity of the complexes was determined in hydroformylation reaction of 1-hexene. Complexes **1** and **2** appeared to be active in isomerisation reactions yielding 76 and 62% of 2-hexene. When used with six-fold excess of triphenylphosphite $P(OPh)_3$ as a modified ligand, the most active catalyst **1** in hydroformylation reaction produced 66% of aldehydes and 22% of 2-hexene.

1. Introduction

In continuation of our studies of coordination abilities of H-spirophosporane ligands, we investigated some palladium(II) and rhenium(V) complexes [1]. Spectroscopic as well as X-ray diffraction studies show that in most cases H-spirophosphorane ligands behave as κ^2 bidentate heterofunctional ligands and coordinate to the metal centre in tautomeric hydroxyalkyl(aryl)phosphite or aminoalkyl(aryl)phosphite form: $[PdCl_2\{P(OCMe_2CMe_2O)OCH_2CMe_2NH_2\}]$ [2], $[PdCl(C_3H_5)\{P(OCMe_2CMe_2O)OCH_2CMe_2NH_2\}]$ [2], *cis*- and *trans*-$[ReOX_2\{P(OCMe_2CMe_2O)OCMe_2CMe_2O\}py]$ [3] (X = Cl, Br, I) $[ReOCl_3\{P(OCH_2CMe_2NH)OCH_2CMe_2NH_2\}]$, $[ReOCl_2\{$-P(OCHMeCHMeO)OCHMeCHMeO}py] [4]. However, the monodentate mode of coordination has also been found. Such coordination propensity has been found for the tetraoxaspirophosphorane ligand $HP(OCMe_2CMe_2O)_2$ in complex $[PdCl(\mu$-Cl)$\{P(OCMe_2CMe_2O)OCMe_2CMe_2OH\}]_2$ [5]. Nevertheless, the same ligand can also coordinate to palladium centre as the bidentate chelating ligand $[Pd\{P(OCMe_2CMe_2O)OCMe_2CMe_2OH\}(CF_3COO)\{P(O)(CMe_2CMe_2O)\}]$ [6]. Furthermore, it has been demonstrated that subtle changes in the H-spirophosphorane structure bonded to transition metals may influence the catalytic activity of the complexes [1]. The fine tuning of H-spirophosphoranes structure connected to the palladium(II) centre catalyst causes evident changes in the yield and selectivity of substituted stilbenes; products of the Heck [5] and Hiyama [2] cross-coupling reactions. The structural effect within coordinated spirophosphorane ligands also finds reflection in the catalytic properties of rhenium complexes. The application of oxo-rhenium(V) spirophosphorane complexes as co-catalysts in aerobic oxidation reaction of aldehydes makes it possible to find a connection between the structure of the complexes and the yield of the products. Although the coordination abilities of H-spirophosphoranes towards rhodium precursor have been studied, little is known, to our knowledge, about the catalytic properties of these complexes [7]. Since rhodium complexes are known to operate as catalysts in hydroformylation reaction, we were curious to determine the relationship between their structure and their catalytic potential; especially as data reported in the literature show that phosphites utilized in hydroformylation process increase catalytic stability, improve reaction rates and selectivities [8].

2. Results and discussion

2.1. Synthesis, spectroscopic characterisation and X-ray structural studies of ligand *L6*

Attempts to obtain rhodium complexes with H-spirophosphorane ligands have focused on various ligands. They are readily obtained in one- or two-stage reactions for symmetrical and unsymmetrical

* Corresponding author. Tel.: +48 71 3757254.
E-mail address: anna.skarzynska@chem.uni.wroc.pl (A. Skarżyńska).

0022-328X/$ – see front matter © 2013 Elsevier B.V. All rights reserved.
http://dx.doi.org/10.1016/j.jorganchem.2013.06.020

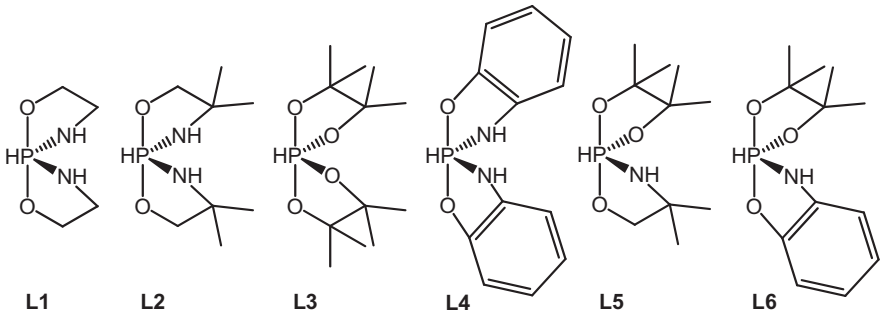

Scheme 1. Drawings of H-spirophosphorane ligands: symmetrical **L1**–**L4** and unsymmetrical **L5**–**L6**.

ligands respectively. The treatment of hexamethylphosphoramide $P(NMe_2)_3$ with diols or aminoalcohols results in the formation of symmetrical compounds: $HP(OCH_2CH_2NH)_2$ **L1** [9], $HP(OCH_2CMe_2NH)_2$ **L2** [10], $HP(OCMe_2CMe_2O)_2$ **L3** [11], $HP(OC_6H_4NH)_2$ **L4** [7], and unsymmetrical compounds: $HP(OCMe_2CMe_2O)(OCH_2CMe_2NH)$ **L5** [2], $HP(OCMe_2CMe_2O)(OC_6H_4NH)$ **L6** (Schemes 1 and 2). Ligand **L6** was obtained in good yield according to the procedure we had previously described for **L5** [2]. The synthesis was conveniently carried out as a single-pot process involving, in the first stage, the formation of $(OCMe_2CMe_2O)PNMe_2$ in equimolar reaction of $P(NMe_2)_3$ with pinacol, and its subsequent reaction with 2-aminophenol to yield $HP(OCMe_2CMe_2O)(OC_6H_4NH)$ **L6**. A doublet at −41.8 ppm with $^1J(P–H) = 823.2$ Hz observed in ^{31}P NMR spectrum, a sensitive tool for the determination of the structural properties of phosphorus compounds, allowed us to determine the exclusive presence of pentacoordinated form of phosphorus moiety with a P–H bond. X-ray data show that the geometry of the **L6** is distorted trigonal bipyramid (TBP) with two oxygen atoms in apical position and third oxygen, nitrogen as well as hydrogen atoms in equatorial positions. Single crystal X-ray diffraction analysis reveals that the stereochemistry of ligand **L6** is nearly identical to what is to be expected from the spectroscopic studies.

The molecular structure of **L6** is shown in Fig. 1. Details of the structural determination are given in Table 1. The bond lengths and angles are broadly similar to those reported for other ligands [12,13]. It is worth mentioning that the P1–O2 bond length of 1.613(2) Å between phosphorus and oxygen atoms located in equatorial positions is shorter than the two other, axial bonds. In the crystal lattice, two adjacent molecules are alternately stabilised by intermolecular hydrogen bonds N–H···O, as reported before for similar ligands [2].

2.2. Synthesis, spectroscopic characterisation and X-ray structural studies of complexes

Using the same rhodium precursor $[Rh(CO)_2Cl]_2$ we were surprised to find that only the bidentate κ^2-P,E (E = N, O) chelating mode of ligand coordination was possible, especially as literature data reported to date show that tetraoxaspirophosphoranes are likely to coordinate to rhodium moiety in monodentate κ^1-P fashion yielding

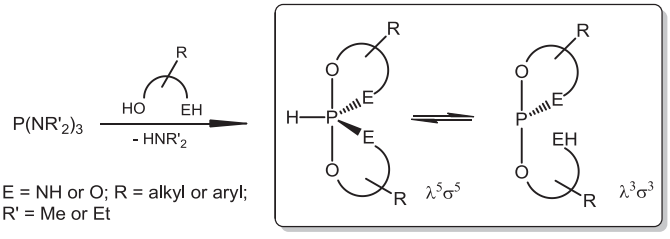

Scheme 2. Synthetic route to H-spirophosphorane ligands.

complexes with dangling hydroxyl group [7,14]. In this study, we demonstrated that all the H-spirophosphoranes **L1**–**L6** are capable of coordinating to the rhodium centre in a tricoordinate hydroxyalkylphosphite or aminoalkyl(aryl)phosphite tautomeric form yielding: $[RhCl(CO)\{P(OCH_2CH_2NH)OCH_2CH_2NH_2\}]$ **1**, $[RhCl(CO)\{P(OCH_2CMe_2NH)OCH_2CMe_2NH_2\}]$ **2**, $[RhCl(CO)\{P(OCMe_2CMe_2O)OCMe_2CMe_2OH\}]$ **3** $[RhCl(CO)\{P(OC_6H_4NH)OC_6H_4NH_2\}]$ **4**, $[RhCl(CO)\{P(OCMe_2CMe_2O)OCH_2CMe_2NH_2\}]$ **5**, $[RhCl(CO)\{P(OCMe_2CMe_2O)OC_6H_4NH_2\}]$ **6** in spite of the fact that all free ligands exist only in pentacoordinate form at 20 °C [15]. The H-spirophosphoranes reacted with the rhodium precursor via the chloride bridge splitting pathway, yielding mononuclear tetra-coordinated rhodium complexes (Scheme 3). In the course of our study we were unfortunately unable to isolate complex **4** in a pure form. To get inside the course of the synthesis of **4**, the reaction was performed in deuterated toluene in an NMR tube and monitored by means of ^{31}P NMR spectroscopy. At ambient temperature, only the doublet corresponding to the free ligand at −47.5 ppm, with $^1J(P–H) = 835$ Hz, is present in the system. The reaction starts at 75 °C, and after 1 h major resonance attributed to rhodium complex **4** (doublet at 140.8 ppm with $^1J(P–Rh) = 287.9$ Hz) along with **L4** as minor resonance signals were detected. After 3 h of heating **L4** was absent in solution; however, apart from product **4**, a singlet at 81.8 ppm, attributed to a new species, and at 13.9 ppm, attributed to some product of ligand decomposition, were also observed. Attempts to get rhodium complexes using other starting materials, e.g. $Rh(acac)(CO)_2$ with ligands **L3** or **L5** even at an elevated temperature (toluene, 75 °C), failed: the unreacted rhodium precursor was still present in the system.

The salient phosphorus nuclear magnetic resonance and infrared spectral data for complexes **1**–**6** are presented in Table 2. IR spectroscopic investigations of the complexes corroborate the ^{31}P NMR findings. The FT-IR spectra of **1**–**6** showed expected

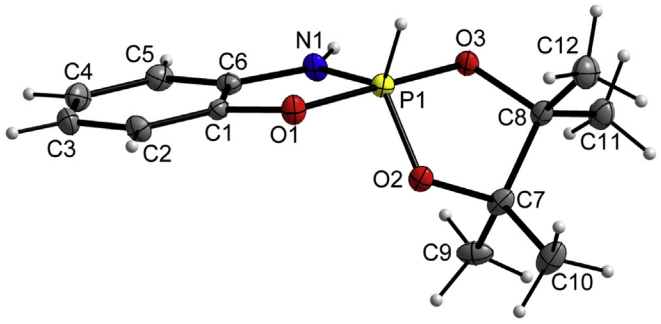

Fig. 1. Molecular structure of ligand **L6**. Displacement ellipsoids are drawn at the 30% probability level and hydrogen atoms are shown as small spheres of arbitrary radii. Selected parameters: P1–O1 1.740(2), P1–O3 1.674(2), P1–O2 1.613(2), P1–N1 1.666(3) Å; O3–P1–O1 178.68(12), O2–P1–N1 124.38(13), N1–P1–O1 88.21(12), O2–P1–O3 92.02(12), O2–P1–O1 87.88(11), N1–P1–O3 90.77(13)°.

Table 1
Crystal data for HP(OCMe$_2$CMe$_2$O)(OC$_6$H$_4$NH) **L6**, [RhCl(CO){P(OCMe$_2$CMe$_2$O)OCMe$_2$CMe$_2$OH}] **3**, [RhCl(CO){P(OCMe$_2$CMe$_2$O)OCH$_2$CMe$_2$NH$_2$}] **5**, [RhCl(CO){P(OCMe$_2$CMe$_2$O)OC$_6$H$_4$NH$_2$}] **6**.

	L6	**3**	**5**	**6**
Empirical formula	$C_{12}H_{18}NO_3P$	$C_{13}H_{25}ClO_5PRh$	$C_{11}H_{22}ClNO_4PRh\cdot0.25(C_3H_6O)$	$C_{13}H_{18}ClNO_4PRh\cdot0.5(C_7H_8)$
Formula weight	255.24	430.66	416.15	467.68
Temperature (K)	100(2)	100(2)	100(2)	100(2)
λ (Å)	0.71073	0.71073	0.71073	0.71073
Crystal system	Orthorhombic	Orthorhombic	Triclinic	Monoclinic
Space group	$Pca2_1$	$Pccn$	P − 1	$P2_1/c$
a (Å)	15.482(7)	15.147(3)	9.263(3)	13.239(3)
b (Å)	8.542(4)	17.862(4)	12.906(4)	15.595(4)
c (Å)	9.986(4)	13.569(4)	15.319(5)	19.576(6)
α			70.54(3)	
β			89.34(3)	108.81(3)
γ			87.48(3)	
Volume (Å^3)	1320.6(10)	3671.2(15)	1725.1(10)	3825.8(18)
Z	4	8	4	8
D_{calc} (g cm^{-3})	1.284	1.558	1.602	1.624
μ (mm^{-1})	0.21	1.18	1.25	1.14
$F(000)$	544	1760	848	1896
Crystal size (mm)	0.28 × 0.10 × 0.03	0.17 × 0.14 × 0.11	0.45 × 0.04 × 0.01	0.23 × 0.18 × 0.11
θ range(°)	3.1–36.8	2.9–36.9	2.9–30.0	2.8–30.0
No of collected reflection	18,159	30,959	25,263	29,778
Independent reflection	3783	5115	9502	9485
S	1.00	1.02	1.01	1.00
R_1/wR_2 indices	0.07/0.129	0.048/0.110	0.036/0.047	0.047/0.128
Flack parameter	0.19(14)			

$R_1 = \sum||F_o| - |F_c||/\sum|F_o|$; $wR_2 = \{\sum[w(F_o^2 - F_c^2)^2]/[w(F_o^2))^2]\}^{1/2}$.
$w = 1/[\sigma^2(F_o^2) + (aP)^2]$ where $P = (F_o^2 + 2F_c^2)/3$, a = 0.0438(**L6**); 0.053(**3**); 0.080(**6**).

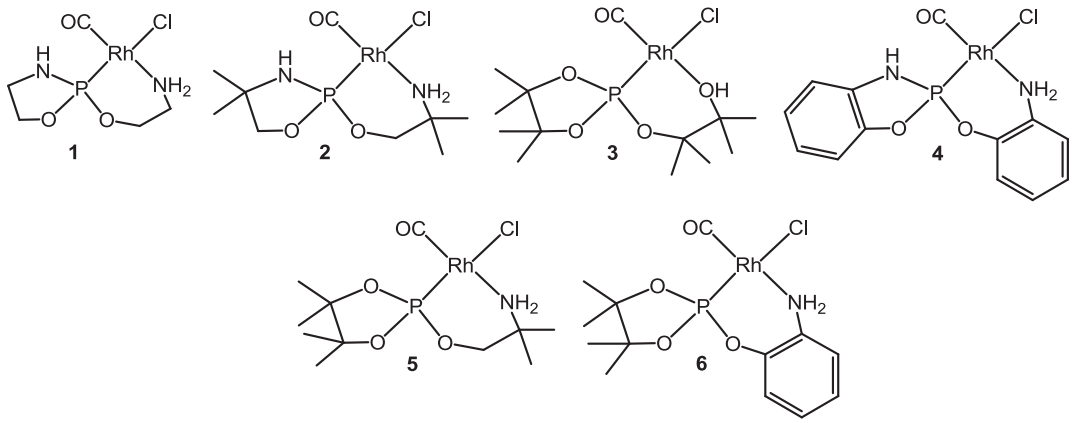

Scheme 3. Rhodium complexes with H-spirophosphorane ligands.

Table 2
Relevant spectroscopic data for metal complexes **1**–**6**.

Complex	$^{31}P\{^1H\}$ NMR[a]			IR[b]		
	δ	^1J(Rh–P)	$\Delta\delta^{31}P\{^1H\}$ NMR[c]	ν(C≡O)	ν(NH$_2$)	ν(Rh–Cl)
1	132.6	243.4	186.1	2002vs	3215s 3274s	293vs
2	135.6	246.1	193.1	2001vs	3127m 3197m	291vs
3	123.2	257.6	163.0	1998vs	–	294vs
4	140.8	287.9	190.2	2025vs[d]	3130[d]	320[d]
5	135.0	264.9	185.0	2012vs	3220m 3253s	298vs
6	147.5	283.6	191.5	2014vs	3209w 3250w	282vs

[a] Spectra recorded in CD_2Cl_2 solution, chemical shift δ in ppm, J(Rh-P) in Hz.
[b] KBr [cm^{-1}].
[c] $\delta^{31}P\{^1H\}$ NMR (complex) − $\delta^{31}P\{^1H\}$NMR (ligand).
[d] Spectrum recorded in $CDCl_3$ [7].

ν(C≡O) stretching frequencies in the range 1998–2025 cm^{-1}. The lowest value was observed for the tetraoxaspirophosphorane complex **3**, and the highest one for complex **4** [7]. The terminal ν(Rh–Cl) stretches for most of the complexes occur near 290 cm^{-1} and are consistent with the configuration having a terminal metal–halogen bond [16].

The bidentate coordination of spirophosphorane moiety corroborates the lack of ν(P–H) stretching vibrations characteristic of free H-spirophosphorane ligands which is usually, located at 2300–2454 cm^{-1} [17], and the presence of narrow bands at approximately 3200 cm^{-1} due to ν(NH$_2$) stretching vibrations for complexes **1**, **2**, **5**, **6** [18]. A protonated bidentate κ^2-P,O mode of ligand **L3** coordination may be inferred from the presence of a broad band at 3109 cm^{-1} attributed to the vibration of ν(OH) [19]. Additional evidence for the presence of a coordinated hydroxyl group in complex **3** is provided by a broad singlet at 4.05 ppm in ^{1}H NMR spectrum. The $^{31}P\{^1H\}$ NMR spectra of **1**–**6** display doublets in the range 123–148 ppm, relevant to rhodium complexes containing a

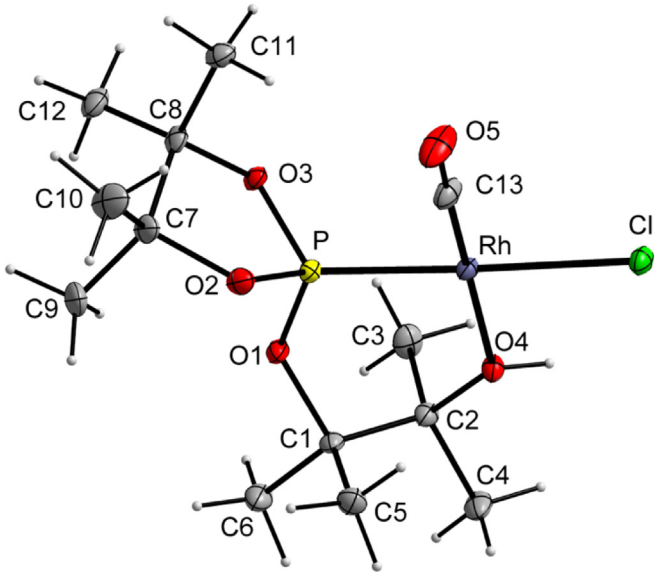

Fig. 2. Molecular structure of complex **3**. Displacement ellipsoids are drawn at the 30% probability level and hydrogen atoms are shown as small spheres of arbitrary radii. Selected parameters: Rh–C13 1.792(4), Rh–P 2.1683(9), Rh–Cl 2.3873(9), Rh–O4 2.108(2) Å; C13–Rh–P 89.79(12), O4–Rh–P 91.65(6), C13–Rh–Cl 91.55(12), O4–Rh–Cl 87.31(6), C13–Rh–O4 174.63(13), P–Rh–Cl 176.47(3)°.

spirophosphorane ligand in κ^2-P,E (E = N, O) form (Table 2). The coordination chemical shifts $\Delta\delta^{31}P\{^1H\}$ NMR exceed the value of 163 Hz and depend on the kind of the coordinated ligand. Large Rh–P coupling values observed for **1**–**6** are analogous to those of known phosphite complexes [20].

From the standpoint of the literature reports, it is possible to find a correlation between the spectroscopic properties of the metal phosphine [21] or phosphite [22] complexes and the electronic properties of phosphorus ligands. Hence, the tentative analysis of the $^{31}P\{^1H\}$ NMR spectroscopic parameters: chemical shifts δ, coupling constants J(Rh–P) or coordination chemical shifts $\Delta\delta^{31}P\{^1H\}$ NMR versus ν(CO) stretching frequencies for complexes **1**–**6** allowed us to determine the relationship between these parameters (Table 2). The ν(CO) values increase in a following order **3** < **2** < **1** < **5** < **6** < **4** and are in line with the decrease in the basicity or electron donor ability of HSP ligands (Figures S1–S3 respectively). In this context ligand **L4** appeared to be the one of the lowest basicity, which consequently may explain the difficulty in obtaining complex **4** in a pure form.

Although there are some examples of spirophosphorane rhodium complexes described in the literature, to the best of our knowledge no crystal structure has so far been reported for any of them. Hence, to corroborate the rhodium coordination environment in complexes **3**, **5** and **6** deduced from spectroscopic measurements, single crystal X-ray diffraction studies were done. Complexes **5** and **6** crystallise with two independent molecules in asymmetric unit. The crystal structures and numbering schemes are illustrated in Figs. 2–4. The X-ray analysis confirms the protonated bidentate behaviour of **L3**, **L5** and **L6** ligands anticipated from spectroscopic studies. The structures are analogous to other structures [23] with almost square planar geometry of metal centre and with phosphorus and chlorine atoms located mutually in a *trans* arrangement. When the rhodium–phosphorus distances are compared with other complexes containing diphosphite ligands, Rh–P distance values are analogues to distances of around 2.16 Å; however, as expected considering the *trans* influence, they are rather short [24].

2.3. Catalytic application

To obtain the information on how electronic effects may influence catalytic activity, we turned our attention on rhodium-catalysed hydroformylation reaction. The methodology of this reaction was utilised as optimised before [25].

The hydroformylation reactions of 1-hexene proceeded under 1 MPa of $CO/H_2 = 1$, at 80 °C in toluene in the presence of catalyst precursors **1**–**6** (Scheme 4).

In the case of complex **4**, we studied in situ formed catalyst, for which we allowed ligand **L4** and catalyst precursor $[Rh(CO)_2Cl]_2$ to react for 30 min in toluene at r.t. prior to the catalytic reaction. The obtained results showed that when complexes **1**–**6** were used alone, the concurrent isomerisation reaction appeared to be dominant, yielding less reactive 2-hexene (Fig. 5). The most

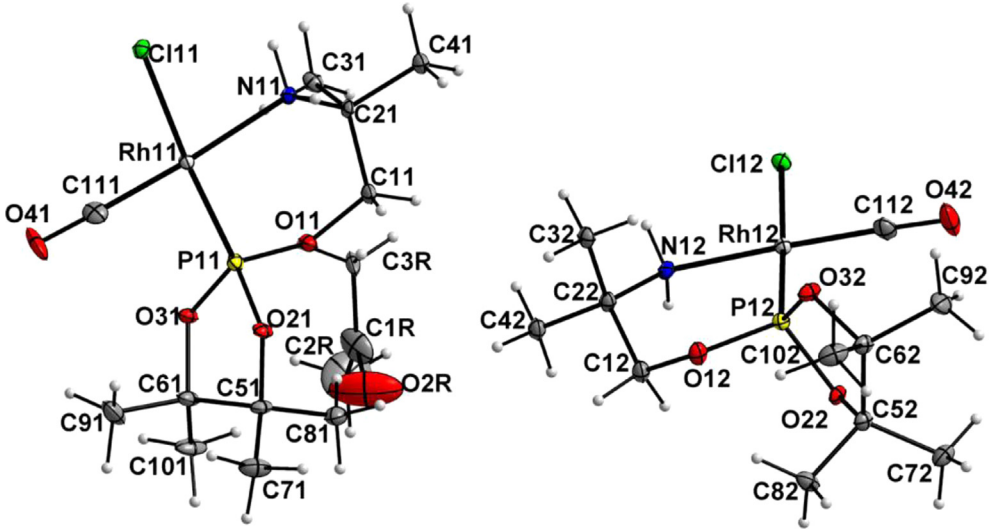

Fig. 3. Molecular structure of complex **5**. Displacement ellipsoids are drawn at the 30% probability level and hydrogen atoms are shown as small spheres of arbitrary radii. Selected parameters: Rh11–C111 1.827(3), Rh12–C112 1.828(3), Rh11–Cl11 2.3902(11), Rh12–Cl12 2.3884(12), Rh11–P11 2.1655(11), Rh12–P12 2.1615(11), Rh11–N11 2.127(2), Rh12–N12 2.129(2) Å; C111–Rh11–N11 176.42(12), C112–Rh12–N12 175.79(12), C111–Rh11–P11 89.67(10), C112–Rh12–P12 88.15(10), C111–Rh11–Cl11 93.72(10), C112–Rh12–Cl12 93.13(10), N11–Rh11–P11 93.08(7), N12–Rh12–P12 93.97(7), N11–Rh11–Cl11 83.64(7), N12–Rh12–Cl12 84.82(7), P11–Rh11–Cl11 175.67(3), P12–Rh12–Cl12 178.36(3)°.

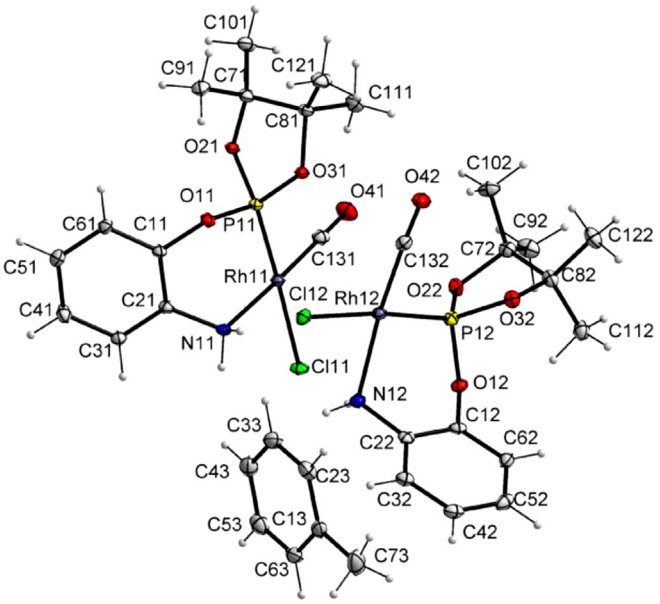

Fig. 4. Molecular structure of complex **6**. Displacement ellipsoids are drawn at the 30% probability level and hydrogen atoms are shown as small spheres of arbitrary radii. Selected parameters: Rh11–C131 1.831(4), Rh12–C132 1.827(3), Rh11–Cl11 2.4039(9), Rh12–Cl12 2.3765(9), Rh11–P11 2.1721(9), Rh12–P12 2.1684(10), Rh11–N11 2.142(3), Rh12–N12 2.151(3) Å; C131–Rh11–N11 177.07(13), C132–Rh12–N12 172.49(13), C131–Rh11–P11 91.51(10), C132–Rh12–P12 90.56(11), C131–Rh11–Cl11 92.46(10), C132–Rh12–Cl12 93.16(11), N11–Rh11–P11 88.47(7), N12–Rh12–P12 88.95(8), N11–Rh11–Cl11 87.62(7), N12–Rh12–Cl12 86.74(8), P11–Rh11–Cl11 175.91(3), P12–Rh12–Cl12 174.01(3)°.

efficient catalyst was complex [RhCl(CO){P(OCH_2CH_2NH)$OCH_2CH_2NH_2$}] **1**, producing up to 76% of 2-hexene and 8% of aldehydes: linear (1-heptanal) and branched (2-methylhexanal and 2-ethylpentanal). Comparable amounts of 1-hexene isomerisation product, i.e. 62% of 2-hexene, were also achieved in reaction catalysed by complex **2**. Remaining complexes, **3**–**6**, appeared to be less active, and only 21% of 2-hexene was produced in a case of complexes **4** and **5**. In the presence of complexes **3** and **6**, hydroformylation yielded the lowest amounts of 2-hexene, 10 and 8% respectively. Keeping in mind that phosphorus ligands, i.e. phosphines or phosphites, added to the system can significantly improve the yield of aldehydes [26], further experiments were performed in the presence of triphenylphosphine, PPh_3. Surprisingly the addition of the phosphine ligand to the system involving complex **1**, (P/Rh = 6) dramatically decreases the yield of aldehydes to nearly 7%; likewise, the addition of H-spirophosphorane suppresses the yield to 3%. However, the addition of triphenylphosphite, $P(OPh)_3$ to the system seemed to play a beneficial role, considerably increasing the amount of aldehydes: for complex **1** to

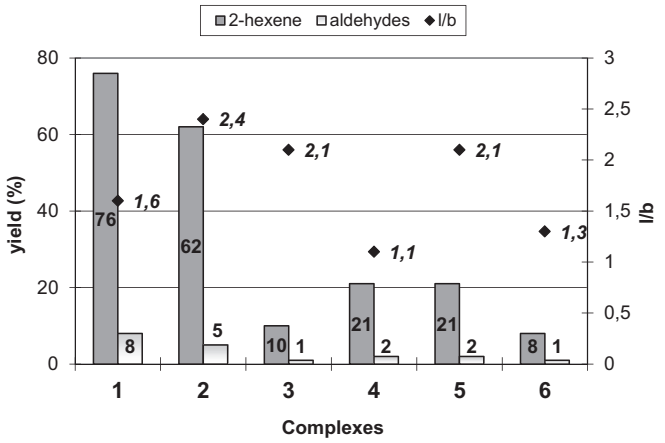

Fig. 5. Results of the hydroformylation of 1-hexene catalysed by the rhodium complexes **1**–**6**; the left axis describes yield (%) of the products; the right axis describes the linear-to-branched-aldehydes ratio (l/b).

66% with regioselectivity (l/b = 7) (Fig. 6). Satisfactory results were also achieved for complexes **2** and **5** with high l/b ratio more than 5. However, once again in the case of complex **3** the results were unsatisfactory: only 13% of 2-hexene and 1% of aldehydes were achieved.

Trying to understand the course of the hydroformylation of 1-hexene, the non-volatile components remaining after the distillation of olefins and aldehydes were analysed by means of $^{31}P\{^1H\}$ NMR technique [27]. Apart from a broad singlet at 127.9 ppm, relevant for $P(OPh)_3$, the spectrum shows a pattern consistent with an A_2BX system, were A, B = ^{31}P; X = ^{103}Rh [20a,28]. The spectrum reveals a double triplet at 118.9 ppm with J(Rh–P) = 285.3 Hz for phosphorus ligands located in the *trans* position, a double doublet at 112.1 ppm with J(Rh–P) = 222.1 Hz for phosphorus ligands located in *cis* position, and coupling constant J(P–P) of 53.0 Hz and 53.5 Hz respectively. It was presumed that under catalytic reaction conditions in the presence of an excess of triphenylphosphite, coordinated spirophosphorane and carbon monoxide ligands were substituted with three molecules of $P(OPh)_3$ yielding the trisphosphite complex [Rh{$P(OPh)_3$}$_3$Cl]. Thus we decided to evaluate the catalytic activity of this species and performed two experiments. In the first one as a source of catalyst we used $[Rh(CO)_2Cl]_2$ in the presence of six-fold excess of $P(OPh)_3$, in the second one [Rh{$P(OPh)_3$}$_3$Cl] alone. In both cases the yield of aldehydes was almost the same (42% and 44%; l/b 6 and 5.3). However, the amount of 2-hexene was higher for complex [Rh{$P(OPh)_3$}$_3$Cl] (47% versus 11%). Although the final product appeared to be the stable complex [Rh{$P(OPh)_3$}$_3$Cl], the resulting amounts of aldehydes: linear and branched, were different for various systems. Hence, in our opinion we cannot rule out the

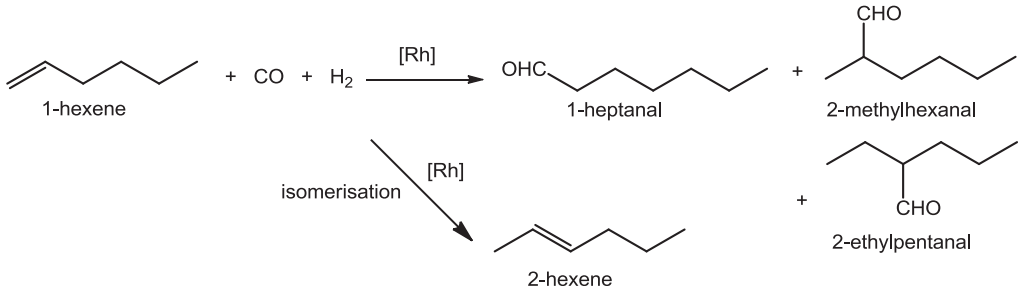

Scheme 4. Products of the hydroformylation reaction of 1-hexene: more desired linear (1-heptanal) and branched (2-methylhexanal, 2-ethylpentanal) aldehydes, along with product of concurrent isomerisation reaction i.e. 2-hexene.

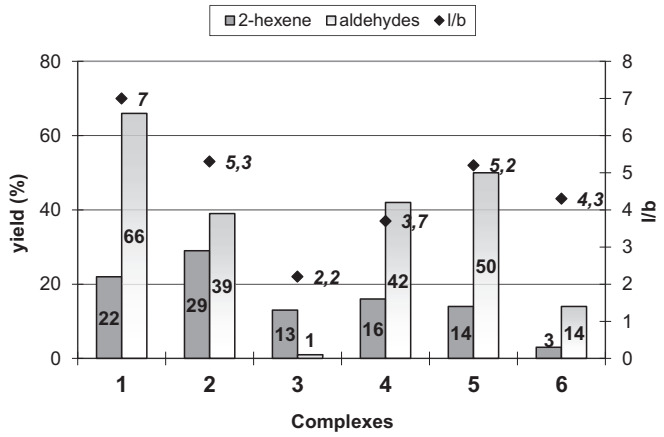

Fig. 6. Results of hydroformylation of 1-hexene catalysed by rhodium complexes **1**–**6** modified with triphenylphosphite $P(OPh)_3$, P/[Rh] = 6; the left axis describes yield (%) of the products, right axis describes the linear-to-branched-aldehydes ratio (l/b).

possibility that rhodium complexes incorporating H-spirophosphorane ligands along with the triphenylphosphite ligand can participate in catalytic cycle. The stability of these complexes under hydroformylation reaction conditions may have a pronounced effect on the course of the catalytic process. This tentative conclusion was drawn based on the observation that when complex [RhCl(CO){P(OCMe$_2$CMe$_2$O)OCMe$_2$CMe$_2$OH}] **3** reacted with an equimolar amount of $P(OPh)_3$, new species were formed within 1.5 h. Apart from uncoordinated **L3**, a new phosphorus species at 9.4 ppm and complex [Rh(CO)Cl{$P(OPh)_3$}$_2$] [20a,29] were detected in $^{31}P\{^1H\}$ NMR spectrum. Moreover, the downfield range of the spectrum also consists of two doublets, at 121.4 and 128.08 ppm, with J(Rh–P) equal to 208.0 and 199.5 Hz, pertinent to two magnetically non-equivalent phosphorus atoms, probably belonging to coordinated $P(OPh)_3$ and **L3** ligands. Quite different observations were made when the more active complexes **5** and **1** reacted with $P(OPh)_3$. The complexes appeared to be more labile and the substitution reaction in both cases immediately led to the decomposition of coordinated spirophosphorane ligands and the formation of the new phosphorus species at 12.1 ppm (**5**) and 1.3 ppm (**1**) respectively. Considering the electronic properties of the coordinated spirophosphorane ligands, in our opinion it is hard to find a correlation between this factor and the catalytic activity of the complexes, though complex **3** incorporating supposedly the most basic ligand HP(OCMe$_2$CMe$_2$O)$_2$ **L3** exhibits the lowest catalytic activity.

Our subsequent efforts were directed towards determining the active form of catalyst present in a system without triphenylphosphite. Therefore, a deuterated toluene solution of the catalyst **5** was heated (353 K) under 1 MPa of CO/H_2 (1:1) for 4 h and analysed by means of $^{31}P\{^1H\}$ NMR spectroscopy. The presence of a doublet at 135.3 ppm and a singlet at 13.10 ppm observed for the post-reaction mixture, attributed to catalyst **5** and the spirophosphorane ligand decomposition product respectively, apart from high yields of isomerisation products, i.e. 2-hexene obtained in the hydroformylation reaction, may suggest that some amounts of the rhodium carbonyl complexes $Rh_6(CO)_{16}$, $Rh_4(CO)_{12}$ are also formed during the catalytic process [30]. The presence of rhodium carbonyl complexes known to produce 2-hexene with 70–90% yield [31], was additionally evidenced by the IR spectrum of the post-reaction solution.

3. Conclusions

To determine the impact of coordinated H-spirophosphoranes on their catalytic activity, a series of rhodium(I) complexes with ligands incorporating variety of peripheral groups were obtained. In addition to symmetrical ligands, also unsymmetrical ones were synthesised to determine the preferences in their coordination modes. It was established that rhodium complexes exclusively exhibit κ^2-P,E (E = N, O) bidentate coordination fashion, and κ^1-P coordination fashion for the tetraoxaspirophosporane ligand, postulated in the literature, was not observed. Some of the complexes appeared to be effective catalysts for the isomerisation of 1-hexene, producing 2-hexene in high yield. However, in the presence of a modifying ligand $P(OPh)_3$, the same complexes turn out to be regioselective catalysts for 1-hexene hydroformylation. The introduction of triphenylphosphite to the system suppressed the isomerisation of 1-hexene and caused an increase in the amount of aldehydes. It was observed that even small changes in ligand structure affect the activity and regioselectivity of the catalytic system, but it is difficult in our opinion to find the systematic correlation between catalytic properties and electronic properties of H-spirophosphorane ligands.

4. Experimental section

4.1. General procedure

Chemicals and deuterated solvents were purchased from Sigma–Aldrich and Fluka and used as received. All preparations were performed in an atmosphere of dry, oxygen-free nitrogen, using conventional Schlenk techniques. Solvents were carefully dried and deoxygenated by standard methods [32]. The ligand precursors 1,6-dioxa-4,9-diaza-5λ^5-phosphaspiro[4.4]nonane HP(OCH$_2$CH$_2$NH)$_2$ **L1** [9], 3,3,8,8-tetramethyl-1,6-dioxa-4,9-diaza-5λ^5-phosphaspiro[4.4]nonane HP(OCH$_2$CMe$_2$NH)$_2$ **L2** [10], 2,2,3,3,7,7,8,8-octamethyl-1,4,6,9-tetraoxa-5λ^5-phosphaspiro[4.4]nonane HP(OCMe$_2$CMe$_2$O)$_2$ **L3** [11], 2λ^5-2,2′-(3*H*,3′*H*)-spirobi[1,3,2-benzoxazaphosphole] HP(OC$_6$H$_4$NH)$_2$ **L4** [7], 2,2,3,3,8,8-hexamethyl-1,4,6-trioxa-9-aza-5λ^5-phosphaspiro[4.4]nonane HP(OCMe$_2$CMe$_2$O)(OCH$_2$CMe$_2$NH) **L5** [2], were prepared according to the literature methods. [RhCl$_2${P(OCH$_2$CMe$_2$NH)OCH$_2$CMe$_2$NH$_2$}] **2** and [RhCl(CO){P(OC$_6$H$_4$NH)OC$_6$H$_4$NH$_2$}] **4** were obtained in a manner described previously [7].

IR and FIR measurements were performed in KBr or Nujol with a Bruker 113V FTIR. ^1H and $^{31}P\{^1H\}$ NMR spectra were obtained on a Bruker AMX (300 MHz for ^1H NMR) or Bruker Avance 500 MHz spectrometer (500 MHz for ^1H NMR). The chemical shifts (δ) are given in ppm towards TMS (^1H) and H_3PO_4 (^{31}P) using deuterated solvents as lock and reference (^1H) respectively. Elemental analyses were performed on a 2400 CHNS Vario EL III apparatus. Analytical gas chromatographic (GC) analyses were performed on a Hewlett Packard 8452A.

4.2. Synthesis of the ligand HP(OCMe$_2$CMe$_2$O)(OC$_6$H$_4$NH) *L6*

4′,4′,5′,5′-tetramethylspiro-[1,3,2-benzoxazaphosphole]-2(3*H*),2′λ^5-[1,3,2]dioxaphospholane HP (OCMe$_2$CMe$_2$O)(OC$_6$H$_4$NH) **L6** was obtained using the general procedure described in the literature for ligand **L5** [2]. The crude product was purified by recrystallisation from hexane in a freezer providing crystals suitable for X-ray analysis.

Anal. Calc. for $C_{12}H_{18}NO_3P$: C, 56.47; H, 7.11; N, 5.49; Found: C, 54.84; H, 7.13; N, 5.20%; ^1H NMR (CD_2Cl_2) δ 1.26, 1.27, 1.29, 1.32 (12H, s's, C*H*$_3$), 5.18 (1H, d, ^2J(P, H) = 17.8 Hz, N*H*), 6.70 (4H, m, Ph-*H*) 7.97 (1H, d ^1J(P, H) = 823.2 Hz, P*H*); ^{31}P NMR (CD_2Cl_2) δ −41.8 (d ^1J(P, H) = 823.2 Hz); IR ν_{max}(nujol)/cm^{-1} 743vs, 949vs, 977vs, 1009m, 1145s ν(C–O–P), 2374m, 2397m ν(P–H), 3370s ν(N–H).

4.3. Synthesis of the complexes

4.3.1. [RhCl(CO){P(OCH$_2$CH$_2$NH)OCH$_2$CH$_2$NH$_2$}] **1**

[Rh(CO)$_2$Cl]$_2$ (0.05 g, 0.13 mmol) was added to a solution of HP(OCH$_2$CH$_2$NH)$_2$ (0.57 g, 0.38 mmol) in toluene (2 cm^3). The yellow solution was stirred for 30 min to produce an orange precipitate. The obtained product was filtered, washed with hexane and dried *in vacuo*. Yield: 0.04 g (47%). Anal. Calc. for $C_5H_{11}ClN_2O_3PRh$: C, 18.98; H, 3.50; N 8.85; Found: C, 19.41; H, 3.60; N, 8.58%; ^{1}H NMR (CD$_2$Cl$_2$) δ 2.81 (2H, m, C*H*$_2$), 3.12 (2H, wide s, N*H*$_2$), 3.33 (2H, m, C*H*$_2$), 3.89 (1H, d, ^2J(P, H) = 24.08 Hz, N*H*), 4.18 (2H, m, C*H*$_2$), 4.26 (2H, m, C*H*$_2$); IR ν_{max}(KBr)/cm^{-1} 920s, 993s, 1033s, 1059s ν(C–O–P), 2002vs ν(CO), 3138m, 3215m, 3274s ν(N–H$_2$) ν(N–H).

4.3.2. [RhCl(CO){P(OCMe$_2$CMe$_2$O)OCMe$_2$CMe$_2$OH}] **3**

[Rh(CO)$_2$Cl]$_2$ (0.07 g, 0.18 mmol) was added to a solution of HP(OCMe$_2$CMe$_2$O)$_2$ (0.10 g, 0.37 mmol) in diethyl ether (15 cm^3). The yellow solution was stirred for 30 min and the excess of the solvent was concentrated *in vacuo* affording a light-yellow precipitate of **3**. The product was filtered, washed with hexane and dried *in vacuo*. Yield: 0.11 g (70%). The crude product was purified by recrystallisation from acetonitrile/toluene/ethyl ether solution, providing crystals suitable for X-ray analysis. Anal. Calc. for $C_{13}H_{25}ClO_5PRh$: C, 36.26; H, 5.85; Found: C, 36.51; H, 5.67%; ^{1}H NMR (CD$_2$Cl$_2$) δ 1.34, 1.40, 1.45, 1.59 (24H, s's, C*H*$_3$), 4.05 (1H, br s, OH); IR ν_{max}(KBr)/cm^{-1} 925vs, 953vs, 1138s ν(C–O–P), 1998vs ν(CO), 3109m, ν(OH).

4.3.3. [RhCl(CO){P(OCMe$_2$CMe$_2$O)OCH$_2$CMe$_2$NH$_2$}] **5**

The complex **5** was prepared in the manner described for **3**, replacing **L3** with the appropriate H-spirophosphorane ligand **L5**. Yield: 0.09 g (50%). The crude product was purified by recrystallisation from dichloromethane/ethyl ether solution, providing crystals suitable for X-ray analysis. Anal. Calc. for $C_{11}H_{22}ClNO_4PRh$: C, 32.90; H, 5.52; N 3.49; Found: C, 32.90; H, 5.46; N, 3.47%; ^{1}H NMR (CD$_2$Cl$_2$) δ 1.22, 1.34, 1.40, (9H, s's, C*H*$_3$), 2.60 (1H, br s, N*H*$_2$), 3.82 (1H, d, ^3J(P, H) = 18.7 Hz, C*H*$_2$); IR ν_{max}(KBr)/cm^{-1} 917vs, 952s, 1047s, 1138s ν(C–O–P), 2012vs ν(CO), 3220m, 3253m ν(N–H$_2$).

4.3.4. [RhCl(CO){P(OCMe$_2$CMe$_2$O)OC$_6$H$_4$NH$_2$}] **6**

Complex **6** was prepared in a manner described for **1**, replacing **L1** with the appropriate H-spirophosphorane ligand **L6**. Yield: 0.09 g (83%). The crude product was purified by recrystallisation from acetonitrile/toluene solution in a freezer, providing crystals suitable for X-ray analysis. Anal. Calc. for $C_{13}H_{18}ClNO_4PRh$: C, 37.03; H, 4.30; N 3.32; Found: C, 38.11; H, 4.42; N, 3.31%; ^{1}H NMR (CD$_2$Cl$_2$) δ 1.40, 1.61 (12H, s's, C*H*$_3$), 4.49 (2H, br s, N*H*$_2$), 7.16 (4H, m, Ar–*H*); IR ν_{max}(KBr)/cm^{-1} 925vs, 956s, 1135s ν(C–O–P), 2014vs ν(CO), 3209w, 3250w ν(N–H$_2$).

4.4. Hydroformylation reaction

Hydroformylation reactions were performed in a steel autoclave with 40 cm^3 Teflon liner under the starting pressure of 1 MPa of H$_2$:CO (1:1). The reactor was charged in an atmosphere of nitrogen with the catalyst precursor (1.5×10^{-5} mol) and an appropriate amount of triphenylphosphite P(OPh)$_3$ or triphenylphosphine PPh$_3$ (if necessary), which were weighed in small Teflon vessels and introduced to the autoclave. Then, dried toluene (1.5 cm^3) and 1-hexene (1.5 cm^3, 1.2×10^{-2} mol) were added. The autoclave was closed, purged with dihydrogen and filled with 5 atm of H$_2$ and 5 atm of CO. The autoclave was heated to 80 °C and reaction mixture was stirred magnetically. After 4 h the autoclave was cooled and opened. The products were separated from the catalyst by vacuum distillation and analysed by GC (or GC–MS).

4.5. Crystal structure determinations

The data were collected on a KM4CCD diffractometer and corrected for Lorentz and polarisation effects. Data reduction was carried out using the Crysalis (Agilent) programs. The structures were solved by the direct method using SHELXS and refined by the full-matrix least-squares method on F^2 using the SHELXL software [33]. Non-hydrogen atoms were refined with anisotropic thermal parameters. Hydrogen atoms were set in calculated positions and refined using the riding model with a common fixed isotropic thermal parameter. The hydrogen atom attached to phosphorus in **L6** was located in a difference Fourier map and its coordinates were freely refined but its displacement parameters were constrained to ride on P atom, with $U_{iso}(H) = 1.5U_{eq}(P)$.

Acknowledgements

Financial support of the National Science Centre (Grant 2012/05/B/ST5/00265) is gratefully acknowledged. The authors are grateful to Mr Przemysław Wójcik for preparing some rhodium complexes.

Appendix A. Supplementary material

CCDC 930868–930870, 934086 contain the supplementary crystallographic data for compounds: **L6**, **3**, **5** and **6** respectively. These data can be obtained free of charge from The Cambridge Crystallographic Data Centre via www.ccdc.cam.ac.uk/data_request/cif.

Appendix B. Supplementary material

Supplementary material associated with this article can be found, in the online version, at http://dx.doi.org/10.1016/j.jorganchem.2013.06.020.

References

[1] A. Skarżyńska, Coord. Chem. Rev. 257 (2013) 1039–1048.
[2] A. Skarżyńska, A. Gniewek, J. Organomet. Chem. 696 (2011) 2985–2992.
[3] W.K. Rybak, A. Skarżyńska, L. Szterenberg, Z. Ciunik, T. Głowiak, Eur. J. Inorg. Chem. (2005) 4964–4975.
[4] A. Skarżyńska, M. Siczek, J.M. Sobczak, Eur. J. Inorg. Chem. (2012) 3331–3341.
[5] A. Skarżyńska, A.M. Trzeciak, M. Siczek, Inorg. Chim. Acta 365 (2011) 204–210.
[6] Li B. Han, Y. Ono, S. Shimada, J. Am. Chem. Soc. 130 (2008) 2752–2753.
[7] K.N. Gavrilov, A.V. Korostylev, A.I. Polosukhin, O.G. Bondarev, A.Yu. Kovalevsky, V.A. Davankov, J. Organomet. Chem. 613 (2000) 148–158.
[8] P.W.M. van Leeuwen, C. Claver (Eds.), Rhodium Catalyzed Hydroformylation, Kluwer Academic Publisher, Dordrecht, 2001.
[9] R. Burgada, Ann. Chim. (Paris) 8 (1963) 347.
[10] A.V. Korostylev, O.G. Bondarev, K.A. Lyssenko, A.Yu. Kovalevsky, P.V. Petrovskii, G.V. Tcherkaev, I.S. Mikhel, V.A. Davankov, K.N. Gavrilov, Inorg. Chim. Acta 295 (1999) 164–170.
[11] D.L. Haire, E.G. Janzen, I. Hrvoic, Magn. Reson. Chem. 37 (1999) 767–773.
[12] P.F. Meunier, R.O. Day, J.R. Devillers, R.R. Holmes, Inorg. Chem. 17 (1978) 3270–3276.
[13] M.G. Newton, J.E. Collier, R. Wolf, J. Am. Chem. Soc. 96 (1974) 6888–6892.
[14] (a) K.N. Gavrilov, Zh. Neorg. Khim. 39 (1994) 1661–1662;
(b) K.N. Gavrilov, I.S. Mikhel, Russ. Chem. Rev. (Engl. Transl.) 65 (1996) 225–247.
[15] R. Burgada, C. Laurenco, J. Organomet. Chem. 66 (1974) 255–270.
[16] Y.M. Frolov, Platinum Metals Rev. 40 (1996) 8–18.
[17] IR ν(P–H)(nujol)/cm^{-1} for: **L1** 2300s, 2371m; **L2** 2339s, 2366s; **L3** 2383m; **L4** 2410w, 2454m; **L5** 2362s; **L6** 2374w, 2397w.
[18] M.A. Garralda, R. Hernandez, L. Ibarlucea, E. Pinilla, M.R. Torres, M. Zarandona, Inorg. Chim. Acta 357 (2004) 2818–2826.
[19] J. Duran, D. Oliver, A. Polo, J. Real, J. Benet-Buchholz, X. Fontrodona, Tetrahedron: Asymm. 14 (2003) 2529–2538.
[20] (a) M. Li Wu, M.J. Desmond, R.S. Drago, Inorg. Chem. 18 (1979) 679–686;
(b) K.N. Gavrilov, O.G. Bondarev, R.V. Lebedev, A.A. Shiryaev, S.E. Lyubimov, A.I. Polosukhin, G.V. Grintselev-Knyazev, K.A. Lyssenko, S.K. Moiseev, N.S. Ikonnikov, V.N. Kalinin, V.A. Davankov, A.V. Korostylev, H.J. Gais, Eur. J. Inorg. Chem. (2002) 1367–1376.
[21] (a) C.A. Tolman, Chem. Rev. 77 (1977) 313–348;
(b) T.T. Derencsényi, Inorg. Chem. 20 (1981) 665–670.

[22] A.M. Trzeciak, H. Bartosz-Bechowski, Z. Ciunik, K. Niesyty, J.J. Ziółkowski, Can. J. Chem. 79 (2001) 752–759.
[23] E. Fernandez, A. Ruiz, C. Claver, S. Castillón, A. Paolo, J.F. Piniella, A. Alvarez-Larena, Organometallics 17 (1998) 2857–2864.
[24] (a) R. Meijboom, A. Muller, A. Roodt, Acta Crystallogr. E60 (2004) m455–m457;
(b) D. Bondoux, B.F. Mentzen, I. Tkatchenko, Inorg. Chem. 20 (1981) 839–848;
(c) D.P. Allen, C.M. Crudden, L.A. Calhoun, R. Wang, A. Decken, J. Organomet. Chem. 690 (2005) 5736–5746;
(d) S. Yanagisawa, T. Sudo, R. Noyori, K. Itami, J. Am. Chem. Soc. 128 (2006) 11748–11749.
[25] A.M. Trzeciak, J.J. Ziółkowski, T. Lis, R. Choukroun, J. Organomet. Chem. 575 (1999) 87–97.
[26] (a) A.M. Trzeciak, J.J. Ziółkowski, Coord. Chem. Rev. 190 (1999) 883–900;
(b) A.M. Trzeciak, J.J. Ziółkowski, J. Organomet. Chem. 464 (1994) 107–111;
(c) H. Janecko, A.M. Trzeciak, J.J. Ziółkowski, J. Mol. Catal. 26 (1984) 355–361.
[27] The experiment was performed in the presence of catalyst **5**, which is well soluble in most of the organic solvents.
[28] (a) E.N. Yurchenko, L.S. Gracheva, Yu. L. Alt, L.A. Pavliukhina, Koord. Khim. 7 (1981) 930–933;
(b) A.M. Trzeciak, Z. Siatecki, J.J. Ziólkowski, Trans. Met. Chem. 11 (1986) 458–459.
[29] A. Muller, R. Meijboom, A. Roodt, J. Organomet. Chem. 691 (2006) 5782–5789. $[Rh(CO)Cl\{P(OPh)_3\}_2]$ $^{31}P\{^1H\}$ NMR (toluene-d^8) δ = 113.8 ppm J(Rh-P) = 215.9 Hz; IR (KBr) ν(CO) = 216 cm^{-1}.
[30] (a) J.A. Creighton, B.T. Heaton, J. Chem. Soc. Dalton Trans. (1981) 1498–1500;
(b) A.D. Allian, M. Garland, Dalton Trans. (2005) 1957–1965.
[31] E. Mieczyńska, A.M. Trzeciak, J.J. Ziółkowski, J. Mol. Catal. 73 (1992) 1–8.
[32] D.D. Perrin, W.L.F. Armarego, Purification of Laboratory Chemicals, third ed., Pergamon Press, Oxford, 1998.
[33] G.M. Sheldrick, Acta Crystallogr. A64 (2008) 112–122.